NATIONAL ADVISORY COMMITTEE FOR AERONAUTICS

TECHNICAL NOTE 4218

ANALYSIS OF STRESSES AND DEFLECTIONS IN A DISK SUBJECTED TO GYROSCOPIC FORCES

By M. H. Hirschberg and A. Mendelson

Lewis Flight Propulsion Laboratory
Cleveland, Ohio

Washington
March 1958

NATIONAL ADVISORY COMMITTEE FOR AERONAUTICS

TECHNICAL NOTE 4218

ANALYSIS OF STRESSES AND DEFLECTIONS IN A DISK SUBJECTED TO GYROSCOPIC FORCES

By M. H. Hirschberg and A. Mendelson

SUMMARY

The differential equation governing the deflection of a disk of variable thickness subjected to gyroscopic loading is derived. For the case of a disk of constant thickness, solutions are obtained by a finite-difference method for a range of centrifugal loading parameter M from 0 to 50, and the ratio of shaft to disk radii varying from 0.1 to 0.3. Results are presented in dimensionless form suitable for design purposes. The method for solving the problem of a disk of variable thickness with a temperature gradient is also presented.

INTRODUCTION

When the axis of rotation of a disk is itself rotated, forces are set up normal to the disk. These forces, or gyroscopic loads, occur on jet-engine compressor and turbine disks whenever the airplane changes direction either in the air or on the ground. These gyroscopic forces will deflect a disk out of its plane of rotation, induce vibratory bending stresses, and produce a bending moment that will increase the shaft bearing loads. This problem may be even more serious for the high-speed disks used in missiles undergoing high accelerations. Although the stresses thus produced may not themselves be very large, the combined effect of these stresses with the already existing stress distribution may be sufficient in some cases to cause a failure. It is therefore necessary to investigate both the stresses and the deflections of a disk under gyroscopic loading.

By considering the gyroscopic forces and centrifugal forces acting on an element of a disk of variable thickness, the general differential equation describing the deflection is derived. A finite-difference solution of this differential equation is obtained for a constant-thickness disk rotating about its center at a constant angular velocity. The computed deflections and the corresponding stresses are plotted in dimensionless form for a wide range of a centrifugal-loading parameter, and for a number of different ratios of shaft to disk radii.

PROCEDURE

The general differential equation governing the deflection of a disk of variable thickness subjected to gyroscopic loading is derived in appendix B and the solution of this general equation is discussed in RESULTS AND DISCUSSION. In this section the procedure used for obtaining numerical solutions of this equation is presented for the special case of a constant-thickness disk rotating about its center at a constant angular velocity ω and at the same time about a diameter fixed in space at an angular velocity Ω and an angular acceleration $\dot{\Omega}$. (The symbols used in this report are defined in appendix A.) Figure 1 shows such a disk along with the type of loading that results from such rotations.

If the deflection at any point such as P is given by w for this disk, and if the dimensionless deflection for a given angle θ is defined by

$$Y = \frac{w}{C}$$

where

$$C = 2m\omega\, a^5 \frac{h}{D}\left(\frac{\dot{\Omega}}{2\omega\Omega}\sin\theta + \cos\theta\right) \tag{1}$$

and m, a, h, and D are the mass density, rim radius, disk thickness, and flexural rigidity, respectively, and θ is the angular coordinate on the face of the disk measured from the diameter about which the disk is rotating, the general differential equation (B19) describing the dimensionless deflection Y becomes

$$Y'''' + \frac{2}{\rho}Y''' - \left[\frac{3}{\rho^2} + M(1-\rho^2)\right]Y'' + \left[\frac{3}{\rho^3} - M\left(\frac{1-3\rho^2}{\rho}\right)\right]Y' - \left[\frac{3}{\rho^4} - M\left(\frac{1-3\rho^2}{\rho^2}\right)\right]Y = \rho \tag{2}$$

where ρ is the dimensionless radius defined as the ratio of the radius at any point P to the disk rim radius, and where M is a centrifugal loading parameter defined by

$$M = \frac{3+\nu}{8} m\omega^2 a^4 \frac{h}{D} \tag{3}$$

where ν is Poisson's ratio for the disk material. The primes in equation (2) denote derivatives with respect to ρ.

The boundary conditions used for all the solutions obtained herein are:

(a) The deflection at the shaft is zero.

(b) The slope of the disk at the shaft is zero.

(c) The total shear at the rim is zero.

(d) The radial bending moment at the rim is zero.

The equations expressing these boundary conditions as derived in appendix C are given by

$$\left.\begin{aligned} &\text{At } \rho = \beta \qquad Y = 0 \\ &\text{At } \rho = \beta \qquad Y' = 0 \\ &\text{At } \rho = 1 \qquad Y''' + Y'' - (3 - \nu)Y' - (3 - \nu)Y = 0 \\ &\text{At } \rho = 1 \qquad Y'' + \nu Y' - \nu Y = 0 \end{aligned}\right\} \tag{4}$$

These are by no means the only set of boundary conditions that could be used. For example, if a disk were to have radial rim loading, boundary condition (d) which states that the radial bending moment at the rim is zero would be replaced by one that states that the radial stress at the rim is equal to the known rim load.

The solution of this problem involves the solving of the fourth-order linear differential equation with variable coefficients (eq. (2)) subject to boundary conditions at two points (eq. (4)). For the case where M equals zero, the exact solution can be readily obtained.

For M not equal to zero, recourse must be made to an approximate solution. The method used herein was to reduce the fourth-order differential equation (2) to a set of four first-order differential equations and then to solve these by a Runge-Kutta finite-difference technique as described in appendix D. The method used for satisfying the boundary conditions is also described in appendix D. Once the differential equation (2) is solved along with the chosen boundary-condition equations, the radial and tangential bending stresses σ_R and σ_T on the face of the disk due to the gyroscopic bending moments can be obtained by equations (B20) as

$$\left.\begin{aligned} \sigma_R &= K\left(Y'' + \frac{\nu}{\rho} Y' - \frac{\nu}{\rho^2} Y\right) \\ \sigma_T &= K\left(\nu Y'' + \frac{1}{\rho} Y' - \frac{1}{\rho^2} Y\right) \end{aligned}\right\} \tag{5}$$

where

$$K = -12\, m\omega\Omega \frac{a^3}{h}\left(\frac{\dot{\Omega}}{2\omega\Omega} \sin\theta + \cos\theta\right) \qquad (6)$$

RESULTS AND DISCUSSION

Solutions were obtained using the finite-difference equations derived in appendix D for disks of constant thickness with the centrifugal loading parameter M varying from 0 to 50 and the ratio of shaft to disk radii varying from 0.1 to 0.3. In order to make the calculations for so many cases, a high-speed digital computer was used. For the limiting case of M equal to zero, equation (2) reduces to the case of a stationary disk with normal loading. This problem is solved in closed form in reference 1 (p. 260). Figure 2 shows plots of dimensionless stress against dimensionless radius for both the exact- and finite-difference solutions at this limiting condition of M equal to zero and for various values of β. It can be seen that excellent agreement has been achieved for all the cases investigated.

Figure 3 shows plots of dimensionless stresses and deflections against dimensionless radii. Each of these plots is for one particular value of β and for a range of values of the centrifugal stress parameter M. For a given set of operating conditions and disk geometry, the parameters C, M, and K are calculated from equations (1), (3), and (6), respectively. The stresses and deflections at any point in the disk can then be determined from the curves for the appropriate value of β. It should be noted from this series of figures that the dimensionless stresses and deflections both decrease as M increases. However, the actual stresses and deflections will always increase as M increases. For a given M, the effect of increasing β is to reduce the deflections and stresses as would be expected. These trends can also be seen in figure 4, where the dimensionless stresses at the shaft and the dimensionless deflections at the rim of the disk are plotted against the centrifugal stress parameter M for various values of β. These plots are used to determine the most critical values of stresses and deflections for this type of problem.

For an example of the use of these figures in solving the problem of a parallel-sided disk, consider a disk with a thickness h of 0.50 inch, an outside radius a of 9.0 inches, a shaft radius of 1.35 inches, an angular velocity ω about its center of 2000 radians per second, an angular velocity Ω and acceleration $\dot{\Omega}$ about a diameter of 1 radian per second and zero radians per second per second, respectively, and a mass density for the disk material of 0.0008 lb-sec^2/in.^{4}, Poisson's ratio of 0.3, and a flexural rigidity of 0.345×10^6 pound-inches. By using these values to determine conditions along the radius $\theta = 0$, the

centrifugal stress parameter M (from eq. (3)), the bending stress parameter K (from eq. (6)), and the deflection parameter C (from eq. (1)) are found to be 12.6, 28×10^3, and 0.275, respectively. For the value of M of 12.6 and the calculated value of β of 0.15, the dimensionless stresses at $\rho = \beta$ and the dimensionless deflection at $\rho = 1$ are found from figure 4 to be 0.750, 0.225, and 0.580. When these dimensionless stresses are multiplied by the bending-stress parameter K, the radial and tangential stresses at the shaft are found to be 2000 and 6300 pounds per square inch, respectively. When the dimensionless deflection is multiplied by the deflection parameter C, the maximum rim deflection is found to be 0.016 inch.

It should be pointed out that these computed gyroscopic stresses are always vibratory stresses. As can be seen from the right side of equation (B17), the gyroscopic load is a function of the angle θ and, therefore, as the disk rotates, the load varies with the frequency $\omega/2\pi$. The stresses, therefore, are vibratory stresses also with the frequency $\omega/2\pi$. The complete stress distribution for this disk is obtained by adding these vibratory bending stresses to the stresses due to the centrifugal loading.

Although these calculations have been performed for the special case of a constant-thickness disk, the solutions for the more general equation (B19) for a variable-thickness disk may be performed in a similar way using the same finite-difference approach, the only difference being in the coefficients of the last of the four finite-difference equations (D8) and (D9). The radial and tangential stresses R and T due to the centrifugal loading will have to be calculated in advance by any of the available methods such as in reference 2. It should also be noted that variations of Young's modulus E, due to either temperature or material variations through the disk, can be taken into account very easily by adjusting the flexural rigidity term D.

In making calculations of this type, the problem presents itself concerning what values of Ω and $\dot{\Omega}$ are likely to occur during operation. These values, in general, would be determined by the type of maneuvers the airplane or missile is capable of performing. However, the occurrence of air gusts and ground bumps may produce greater values of Ω and $\dot{\Omega}$. These effects are, of course, difficult to determine but some estimate would have to be made before a reasonably safe analysis could be made.

CONCLUDING REMARKS

The analysis of the gyroscopic loading on a constant-thickness disk has shown how this effect can be considered by the designer. For the case of a uniform-thickness disk, curves are presented that can be used for design purposes. The disk of variable thickness with temperature

gradient requires individual calculation, which can readily be performed by the method outlined in this report.

Lewis Flight Propulsion Laboratory
National Advisory Committee for Aeronautics
Cleveland, Ohio, December 19, 1957

4708

APPENDIX A

SYMBOLS

a	disk radius
C	deflection parameter, $2m\omega\Omega a^5 \frac{h}{D}\left(\frac{\dot{\Omega}}{2\omega\Omega} \sin \theta + \cos \theta\right)$
D	flexural rigidity, $Eh^3/12(1 - \nu^2)$
E	Young's modulus of elasticity
h	disk thickness
K	bending-stress parameter, $-12m\omega\Omega \frac{a^3}{h}\left(\frac{\dot{\Omega}}{2\omega\Omega} \sin \theta + \cos \theta\right)$
M	centrifugal-loading parameter, $\frac{3 + \nu}{8} m\omega^2 a^4 \frac{h}{D}$
m	mass density
q	normal load intensity
R	radial stress due to centrifugal loading
r	radial coordinate of point in disk
T	tangential stress due to centrifugal loading
w	disk deflection, function of ρ and θ
Y	dimensionless disk deflection, function of ρ only
β	ratio of shaft to disk radius
θ	angular coordinate in plane of disk
ν	Poisson's ratio
ρ	dimensionless radius, r/a
σ_R	radial bending stress on face of disk due to gyroscopic loading
σ_T	tangential bending stress on face of disk due to gyroscopic loading
φ	angular displacement of disk about a diameter x - x (fig. 5)
Ω or $\dot{\varphi}$	angular velocity about disk diameter, rad/sec
ω or $\dot{\theta}$	angular velocity about disk center, rad/sec

APPENDIX B

DERIVATION OF DIFFERENTIAL EQUATION FOR DEFLECTIONS OF VARIABLE-THICKNESS DISK SUBJECTED TO GYROSCOPIC LOADING

If it is assumed that the load per unit area q acting on a plate is normal to its surface and that the deflections w are small in comparison with the thickness h of the plate, the equation of equilibrium becomes (ref. 1, p. 85)

$$\frac{\partial^2 M_x}{\partial x^2} + \frac{\partial^2 M_y}{\partial y^2} - 2\frac{\partial^2 M_{xy}}{\partial x \partial y} = -q \tag{B1}$$

where the bending moments M_x, M_y, M_{xy} are given by

$$\left.\begin{aligned} M_x &= -D(w_{xx} + \nu w_{yy}) \\ M_y &= -D(w_{yy} + \nu w_{xx}) \\ M_{xy} &= D(1 - \nu)w_{xy} \end{aligned}\right\} \tag{B2}$$

where ν is Poisson's ratio and D is the flexural rigidity of the plate. The bending stresses on the surface of the plate are

$$\left.\begin{aligned} \sigma_x &= \frac{6M_x}{h^2} \\ \sigma_y &= \frac{6M_y}{h^2} \end{aligned}\right\} \tag{B3}$$

By substituting equations (B2) into equation (B1) and letting D be a function of x and y, equation (B1) becomes

$$D(w_{xxxx} + w_{yyyy} + 2w_{xxyy}) + D_{xx}(w_{xx} + \nu w_{yy}) + D_{yy}(w_{yy} + \nu w_{xx}) +$$

$$2D_x(w_{xxx} + w_{xyy}) + 2D_y(w_{yyy} + w_{xxy}) + 2(1 - \nu)D_{xy}w_{xy} = q \tag{B4}$$

where the subscripts on D and w represent partial derivatives with respect to the subscript. If equation (B4) is converted to polar coordinates and it is assumed that D is only a function of the dimensionless radius ρ, equation (B4) becomes

$$w_{\rho\rho\rho\rho} + 2\left(\frac{1}{\rho} - \frac{D'}{D}\right)w_{\rho\rho\rho} - \left[\frac{1}{\rho^2} - (2 + \nu)\frac{D'}{\rho D} - \frac{D''}{D}\right]w_{\rho\rho} + \left(\frac{1}{\rho^3} - \frac{D'}{\rho^2 D} + \frac{\nu D''}{\rho D}\right)w_{\rho} +$$

$$\frac{2}{\rho^2}w_{\rho\rho\theta\theta} - 2\left(\frac{1}{\rho^3} - \frac{D'}{\rho^2 D}\right)w_{\rho\theta\theta} + \left(\frac{4}{\rho^4} - \frac{3D'}{\rho^3 D} + \frac{\nu D''}{\rho^2 D}\right)w_{\theta\theta} + \frac{1}{\rho^4}w_{\theta\theta\theta\theta} = \frac{qa^4}{D} \tag{B5}$$

where the superscripts on D indicate total derivatives with respect to ρ, and a is the outside radius of the disk. If equations (B2) are substituted into (B3) and conversion to polar coordinates is made, the stress equations become

$$\left.\begin{aligned} \sigma_R &= -\frac{6D}{a^2h^2}\left[w_{\rho\rho} + \nu\left(\frac{1}{\rho}w_{\rho} + \frac{1}{\rho^2}w_{\theta\theta}\right)\right] \\ \sigma_T &= -\frac{6D}{a^2h^2}\left(\frac{1}{\rho}w_{\rho} + \frac{1}{\rho^2}w_{\theta\theta} + \nu w_{\rho\rho}\right) \end{aligned}\right\} \tag{B6}$$

The normal load intensity term q in equation (B5) may be analyzed as being composed of two separate loading terms. The first term, q_1, is due to the so-called "gyroscopic forces," and the second term, q_2, is due to the normal components of the stresses in the plane of the disk when the disk undergoes bending out of this plane (fig. 1). For the derivation of the q_1 term, the coordinate system of figure 5 will be used. For an aircraft or missile making a turn, the turbine or compressor disk is rotating about its axis and at the same time about a diameter fixed in space. Consider a point P on a disk as shown in figure 5. The disk is rotating about its axis and also about a diameter that is at any time coincident with the X-axis. From reference to this figure, it can be seen that the angular velocity ω is equal to $\dot{\theta}$, and the angular velocity Ω equals $\dot{\varphi}$. Also, if it is noted from the figure that the magnitude of the vector r remains constant with time t, the orthonogal components of the acceleration of point P are given by

$$\left.\begin{aligned} A_x &= \frac{rd^2}{dt^2}(\cos\theta) \\ A_y &= \frac{rd^2}{dt^2}(\sin\theta \sin\varphi) \\ A_z &= \frac{rd^2}{dt^2}(\sin\theta \cos\varphi) \end{aligned}\right\} \tag{B7}$$

where θ is the angle between the radius vector and the X-axis, and φ is the angle between the Z-axis and the projection of the radius vector on the YZ-plane. The acceleration of point P normal to the plane of the disk is given by

$$A_n = aA_x + bA_y + cA_z \tag{B8}$$

where a, b, and c are the direction cosines of the normal to the plane of the disk. For this case

$$\left.\begin{aligned} a &= 0 \\ b &= \cos\varphi \\ c &= -\sin\varphi \end{aligned}\right\} \tag{B9}$$

When equations (B7) and (B9) are substituted into equations (B8), the acceleration normal to the disk becomes

$$A_n = r(\ddot{\varphi}\sin\theta + 2\dot{\varphi}\dot{\theta}\cos\theta) \tag{B10}$$

The force per unit area on particle P is then given by

$$q_1 = mhA_n = mhr(\dot{\Omega}\sin\theta + 2\omega\Omega\cos\theta) \tag{B11}$$

For the derivation of the second part of the normal load intensity q_2 due to components of the centrifugal forces when the disk undergoes bending, an element of the disk as shown in figure 6 will be used. Summing up the Z-components of the forces on this element results in the following equation:

$$h_1\left(R + \frac{\partial R}{\partial r}\,dr\right)(r + dr)d\theta\left.\frac{\partial w}{\partial r}\right|_1 - Rrh_2\,d\theta\left.\frac{\partial w}{\partial r}\right|_2 + T\,dr\,\frac{h}{r}\left(\left.\frac{\partial w}{\partial\theta}\right|_3 - \left.\frac{\partial w}{\partial\theta}\right|_4\right) -$$

$$mr\,dr\,d\theta\,h\frac{\partial^2 w}{\partial t^2} = q_2\,r\,dr\,d\theta \tag{B12}$$

where R and T are the centrifugal radial and tangential stresses, respectively, and the numerical subscripts on the thickness h and the partial derivatives of the deflection w represent their values at different locations in the disk element as shown in figure 6. To relate both the thickness and the derivatives of the deflection at points 1, 2, 3, and 4 to a common point at the center of the element, the first two terms of a Taylor series expansion is used, from which

$$\left.\begin{aligned}
\left.\frac{\partial w}{\partial r}\right|_1 &= \frac{\partial w}{\partial r} + \frac{\partial^2 w}{\partial r^2}\frac{dr}{2} \\
\left.\frac{\partial w}{\partial r}\right|_2 &= \frac{\partial w}{\partial r} - \frac{\partial^2 w}{\partial r^2}\frac{dr}{2} \qquad h_1 = h + \frac{\partial h}{\partial r}\frac{dr}{2} \\
\left.\frac{\partial w}{\partial \theta}\right|_3 &= \frac{\partial w}{\partial \theta} + \frac{\partial^2 w}{\partial \theta^2}\frac{d\theta}{2} \qquad h_2 = h - \frac{\partial h}{\partial r}\frac{dr}{2} \\
\left.\frac{\partial w}{\partial \theta}\right|_4 &= \frac{\partial w}{\partial \theta} - \frac{\partial^2 w}{\partial \theta^2}\frac{d\theta}{2}
\end{aligned}\right\} \qquad \text{(B13)}$$

where $h_3 = h_4 = h$. Substituting equations (B13) back into equation (B12), dividing through by $r\,dr\,d\theta$ and dropping higher order terms, results in

$$q_2 = Rh\frac{\partial^2 w}{\partial r^2} + \left(h\frac{\partial R}{\partial r} + \frac{Rh}{r} + R\frac{\partial h}{\partial r}\right)\frac{\partial w}{\partial r} + \frac{Th}{r^2}\frac{\partial^2 w}{\partial \theta^2} - mh\frac{\partial^2 w}{\partial t^2} \qquad \text{(B14)}$$

The term $\partial^2 w/\partial t^2$ in equation (B14) can be written as

$$\frac{\partial^2 w}{\partial t^2} = \left(\frac{\partial \theta}{\partial t}\right)^2\frac{\partial^2 w}{\partial \theta^2} + \frac{\partial^2 \theta}{\partial t^2}\frac{\partial w}{\partial \theta} \qquad \text{(B15)}$$

Substituting equation (B15) into equation (B14) and letting $r = a\rho$ yields

$$q_2 = \frac{Rh}{a^2}w_{\rho\rho} + \frac{1}{a^2}\left(hR' + \frac{hR}{\rho} + h'R\right)w_\rho + \frac{hT}{a^2\rho^2}w_{\theta\theta} - mh(\omega^2 w_{\theta\theta} + \dot{\omega}w_\theta) \qquad \text{(B16)}$$

When equations (B16) and (B11) are added to give the total normal load intensity term q, and this term is substituted into equation (B5) and terms involving like derivatives of w are collected, equation (B5) becomes

$$\begin{aligned}
&w_{\rho\rho\rho\rho} + 2\left(\frac{1}{\rho} + \frac{D'}{D}\right)w_{\rho\rho\rho} - \left[\frac{1}{\rho^2} - (2+\nu)\frac{D'}{\rho D} - \frac{D''}{D} + \frac{hRa^2}{D}\right]w_{\rho\rho} + \\
&\left[\frac{1}{\rho^3} - \frac{D'}{\rho^2 D} + \frac{\nu D''}{\rho D} - \frac{a^2}{D}\left(hR' + \frac{hR}{\rho} + h'R\right)\right]w_\rho + \frac{2}{\rho^2}w_{\rho\rho\theta\theta} - \\
&2\left(\frac{1}{\rho^3} - \frac{D'}{\rho^2 D}\right)w_{\rho\theta\theta} + \left(\frac{4}{\rho^4} - \frac{3D'}{\rho^3 D} + \frac{\nu D''}{\rho^2 D} - \frac{hTa^2}{\rho^2 D} + m\omega^2\frac{ha^4}{D}\right)w_{\theta\theta} + \\
&\frac{1}{\rho^4}w_{\theta\theta\theta\theta} + m\dot{\omega}\frac{a^4 h}{D}w_\theta = 2m\omega\Omega\frac{ha^5}{D}\rho\left(\frac{\dot{\Omega}}{2\omega\Omega}\sin\theta + \cos\theta\right)
\end{aligned} \qquad \text{(B17)}$$

If it is assumed that the disk is rotating about its center at a constant angular velocity during a change in direction of its axis, $\dot{\omega}$ is equal to zero and a solution to equation (B17) may now be assumed to be of the form

$$w = CY \tag{B18}$$

where Y is only a function of the dimensionless radius ρ, and where

$$C = 2m\omega\Omega\, a^5 \frac{h}{D}\left(\frac{\dot{\Omega}}{2\omega\Omega}\sin\theta + \cos\theta\right)$$

Substituting equation (B18) into (B17) results in the total differential equation

$$Y'''' + 2\left(\frac{1}{\rho} + \frac{D'}{D}\right)Y''' - \left[\frac{3}{\rho^3} - (2+\nu)\frac{D'}{\rho D} - \frac{D''}{D} + \frac{hRa^2}{D}\right]Y'' +$$

$$\left[\frac{3}{\rho^3} - \frac{3D'}{\rho^2 D} + \frac{\nu D''}{\rho D} - \frac{a^2}{D}\left(hR' + \frac{hR}{\rho} + h'R\right)\right]Y' -$$

$$\left(\frac{3}{\rho^4} - \frac{3D'}{\rho^3 D} + \frac{\nu D''}{\rho^2 D} - \frac{hTa^2}{\rho^2 D} + m\omega^2\frac{ha^4}{D}\right)Y = \rho \tag{B19}$$

and the stress equations (B6) become

$$\left.\begin{aligned}\frac{\sigma_T}{K} &= \left(\nu Y'' + \frac{1}{\rho}Y' - \frac{1}{\rho^2}Y\right)\\ \frac{\sigma_R}{K} &= \left(Y'' + \frac{\nu}{\rho}Y' - \frac{\nu}{\rho^2}Y\right)\end{aligned}\right\} \tag{B20}$$

where

$$K = \frac{-12m\omega\Omega a^3}{h}\left(\frac{\dot{\Omega}}{2\omega\Omega}\sin\theta + \cos\theta\right) \tag{B21}$$

4708

For a solid disk of constant thickness, the centrifugal radial and tangential stresses are given simply by

$$\left.\begin{aligned} R &= \frac{3+\nu}{8} m\omega^2 a^2 (1-\rho^2) \\ T &= \frac{3+\nu}{8} m\omega^2 a^2 \left(1 - \frac{1+3\nu}{3+\nu}\rho^2\right) \end{aligned}\right\} \tag{B22}$$

where the centrifugal stresses due to the disks rotation about its diameter have been neglected since Ω will always be much smaller than ω for all practical cases. All the derivatives of D and h with respect to ρ are equal to zero and under these conditions, equation (B19) reduces to

$$Y'''' + \frac{2}{\rho} Y''' - \left[\frac{3}{\rho^2} + M(1-\rho^2)\right] Y'' + \left[\frac{3}{\rho^3} - M\left(\frac{1-3\rho^2}{\rho}\right)\right] Y' - \left[\frac{3}{\rho^4} - M\left(\frac{1-3\rho^2}{\rho^2}\right)\right] Y = \rho \tag{B23}$$

where the centrifugal loading parameter M is given by

$$M \equiv \frac{3+\nu}{8} m\omega^2 a^4 \frac{h}{D} \tag{B24}$$

APPENDIX C

BOUNDARY-CONDITION EQUATIONS

A set of four boundary conditions are needed for the solution of the fourth-order differential equation of the deflection of a disk under normal loading. For a freely rotating single disk such as a turbine wheel, the boundary conditions will be taken as follows:

(a) The deflection at the shaft is zero.

(b) The slope of the disk at the shaft is zero.

(c) The total shear at the rim is zero.

(d) The radial bending moment at the rim is zero.

The total shear V is given by (ref. 1, p. 259)

$$V = Q_r - \frac{1}{r}\frac{\partial M_{r\theta}}{\partial \theta} \tag{C1}$$

where

$$\left.\begin{aligned} Q_r &= -D\frac{\partial}{\partial r}\left(\frac{\partial^2 w}{\partial r^2} + \frac{1}{r}\frac{\partial w}{\partial r} + \frac{1}{r^2}\frac{\partial^2 w}{\partial \theta^2}\right) \\ \text{and} \\ M_{r\theta} &= (1-\nu)D\left(\frac{1}{r}\frac{\partial^2 w}{\partial r \partial \theta} - \frac{1}{r^2}\frac{\partial w}{\partial \theta}\right) \end{aligned}\right\} \tag{C2}$$

if equations (C2) are substituted into (C1) and $r = a\rho$ then

$$V = -\frac{D}{a^3}\left(\frac{\partial^3 w}{\partial \rho^3} + \frac{1}{\rho}\frac{\partial^2 w}{\partial \rho^2} - \frac{1}{\rho^2}\frac{\partial w}{\partial \rho} + \frac{2-\nu}{\rho^2}\frac{\partial^3 w}{\partial \rho \partial \theta^2} - \frac{3-\nu}{\rho^3}\frac{\partial^2 w}{\partial \theta^2}\right) \tag{C3}$$

If the total shear is equal to zero at the rim (or $\rho = 1$) equation (C3) becomes

$$0 = \frac{\partial^3 w}{\partial \rho^3} + \frac{\partial^2 w}{\partial \rho^2} - \frac{\partial w}{\partial \rho} + (2-\nu)\frac{\partial^3 w}{\partial \rho \partial \theta^2} - (3-\nu)\frac{\partial^2 w}{\partial \theta^2} \tag{C4}$$

The radial moment is equal to (ref. 1, p. 259)

$$M_r = -D\left[\frac{\partial^2 w}{\partial r^2} + \nu\left(\frac{1}{r}\frac{\partial w}{\partial r} + \frac{1}{r^2}\frac{\partial^2 w}{\partial \theta^2}\right)\right] \tag{C5}$$

If $r = a\rho$ and if this radial moment is equal to zero at the rim, equation (C5) becomes

$$0 = \frac{\partial^2 w}{\partial \rho^2} + \nu\frac{\partial w}{\partial \rho} + \nu\frac{\partial^2 w}{\partial \theta^2} \tag{C6}$$

The last two boundary conditions are given simply by

$$\left.\begin{aligned} w &= 0 \\ \frac{\partial w}{\partial \rho} &= 0 \end{aligned}\right\} \text{ at } \rho = \beta \tag{C7}$$

and

where β is the ratio of the shaft radius to the disk radius.

APPENDIX D

FINITE-DIFFERENCE EQUATIONS

In order to obtain a solution to the general differential equation (B19), it is convenient to reduce this fourth-order equation to a set of four first-order equations as follows; let

$$\left.\begin{aligned} Y' &= J \\ Y'' &= J' = K \\ Y''' &= K' = L \end{aligned}\right\} \tag{D1}$$

and equation (B19) becomes

$$L' = E - AL - BK - CJ - DY \tag{D2}$$

where A, B, C, D, and E are the corresponding coefficients appearing in equation (B19). These equations can now be written in finite-difference form using a simple Runge-Kutta method (ref. 3, p. 233). Consider a section of a disk as shown in figure 7 where there are n equally spaced stations between $\rho = \beta$ and $\rho = 1$. Consider the following Taylor series expansion for Y at the $i + 1$ station in terms of the value of Y at the i station

$$Y_{i+1} = Y_i + \Delta\rho Y_i' + \frac{\Delta\rho^2}{2} Y_i'' + \cdots \tag{D3}$$

If the first three terms of equation (D3) are used and it is assumed that the second derivative is approximated by

$$Y_i'' = \frac{Y_{i+1}' - Y_i'}{\Delta\rho} \tag{D4}$$

equation (D3) reduces to

$$Y_{i+1} = Y_i + \frac{\Delta\rho}{2} (Y_i' + Y_{i+1}') \tag{D5}$$

If the first of equations (D1) is substituted in (D5), equation (D5) becomes

$$Y_{i+1} = Y_i + \frac{\Delta\rho}{2}(J_i + J^*_{i+1})$$

and in a similar manner the values of J, K, and L at the i+1 station are obtained with the aid of equations (D1) and (D2)

$$\left.\begin{aligned} J_{i+1} &= J_i + \frac{\Delta\rho}{2}(K_i + K^*_{i+1}) \\ K_{i+1} &= K_i + \frac{\Delta\rho}{2}(L_i + L^*_{i+1}) \\ L_{i+1} &= L_i - \frac{\Delta\rho}{2}\left[(A_iL_i + B_iK_i + C_iJ_i + D_iY_i) + \right. \\ &\qquad \left.(A_{i+1}L^*_{i+1} + B_{i+1}K^*_{i+1} + C_{i+1}J^*_{i+1} + D_{i+1}Y^*_{i+1})\right] + \\ &\qquad \frac{\Delta\rho}{2}(E_i + E_{i+1}) \end{aligned}\right\} \quad (D6)$$

where the starred exponents represent first approximations to these values. These terms will be obtained from the first two terms of the Taylor series or

$$\left.\begin{aligned} Y^*_{i+1} &= Y_i + \Delta\rho J_i \\ J^*_{i+1} &= J_i + \Delta\rho K_i \\ K^*_{i+1} &= K_i + \Delta\rho L_i \\ L^*_{i+1} &= L_i - \Delta\rho(A_iL_i + B_iK_i + C_iJ_i + D_iY_i) + \Delta\rho E_i \end{aligned}\right\} \quad (D7)$$

If the problem of a solid disk of constant thickness is to be solved, equation (B23) is substituted into the last of equations (D6) and (D7) and the values of Y, J, K, and L at the i+1 station can now be written in terms of the i station as

$$\left.\begin{aligned} Y_{i+1} &= Y_i + \frac{\Delta\rho}{2}(J_i + J^*_{i+1}) \\ J_{i+1} &= J_i + \frac{\Delta\rho}{2}(K_i + K^*_{i+1}) \\ K_{i+1} &= K_i + \frac{\Delta\rho}{2}(L_i + L^*_{i+1}) \\ L_{i+1} &= L_i + \frac{\Delta\rho}{2}\left\{\begin{aligned} &-\frac{2L_i}{\rho_i} + \left[\frac{3}{\rho_i^2} + M(1-\rho_i^2)\right]K_i - \left[\frac{3}{\rho_i^3} - M\left(\frac{1-\rho_i^2}{\rho_i}\right)\right]J_i + \left[\frac{3}{\rho_i^4} - M\left(\frac{1-\rho_i^2}{\rho_i^2}\right)\right]Y_i \\ &-\frac{2L^*_{i+1}}{\rho_{i+1}} + \left[\frac{3}{\rho_{i+1}^2} + M(1-\rho_{i+1}^2)\right]K^*_{i+1} - \left[\frac{3}{\rho_{i+1}^3} - M\left(\frac{1-\rho_{i+1}^2}{\rho_{i+1}}\right)\right]J^*_{i+1} + \left[\frac{3}{\rho_{i+1}^4} - M\left(\frac{1-\rho_{i+1}^2}{\rho_{i+1}^2}\right)\right]Y^*_{i+1} \end{aligned}\right\} + \\ &\frac{\Delta\rho}{2}(\rho_i + \rho_{i+1}) \end{aligned}\right\} \quad \text{(D8)}$$

where the starred terms are given by

$$\left.\begin{aligned} Y^*_{i+1} &= Y_i + \Delta\rho J_i \\ J^*_{i+1} &= J_i + \Delta\rho K_i \\ K^*_{i+1} &= K_i + \Delta\rho L_i \\ L^*_{i+1} &= L_i + \Delta\rho\left\{-\frac{2L_i}{\rho_i} + \left[\frac{3}{\rho_i^2} + M(1-\rho_i^2)\right]K_i - \left[\frac{3}{\rho_i^3} - M\left(\frac{1-\rho_i^2}{\rho_i}\right)\right]J_i + \left[\frac{3}{\rho_i^4} - M\left(\frac{1-\rho_i^2}{\rho_i^2}\right)\right]Y_i\right\} + \Delta\rho(\rho_i) \end{aligned}\right\} \quad \text{(D9)}$$

The solution of the differential equation (B23) has thus been reduced to computation of a set of deflections and corresponding derivatives by means of the recurrance relations (D8) and (D9). It must be remembered that the solutions which satisfy equations (D8) and (D9) must also satisfy the boundary conditions (C8). Such a set of solutions can be obtained in the following manner:

Let $Y^{(1)}$, $J^{(1)}$, $K^{(1)}$, $L^{(1)}$, and $Y^{(2)}$, $J^{(2)}$, $K^{(2)}$, $L^{(2)}$, be two homogeneous solutions for Y, J, K, and L (that is, solutions for eqs. (D8)

and (D9)) with the last terms in the L_{i+1} and L^*_{i+1} expressions, namely $\Delta\rho/2\ (\rho_i + \rho_{i+1})$ and $\Delta\rho(\rho_i)$, respectively, being equal to zero) and let $Y^{(3)}$, $J^{(3)}$, $K^{(3)}$, and $L^{(3)}$ be particular solutions for Y, J, K, and L. Furthermore, let these three solutions satisfy the boundary conditions that $Y = Y' = 0$ at $\rho = \beta$. This corresponds to Y_1 and J_1 being zero. Since equation (B23) and the corresponding finite difference equations (D8) are linear, the complete solution to equations (D8) can be written as

$$\left.\begin{aligned} Y_i &= aY_i^{(1)} + bY_i^{(2)} + Y_i^{(3)} \\ J_i &= aJ_i^{(1)} + bJ_i^{(2)} + J_i^{(3)} \\ K_i &= aK_i^{(1)} + bK_i^{(2)} + K_i^{(3)} \\ L_i &= aL_i^{(1)} + bL_i^{(2)} + L_i^{(3)} \end{aligned}\right\} \tag{D10}$$

where a and b are determined so as to satisfy the two boundary conditions at $\rho = 1$. It should be noted that if the solutions were not chosen in order to satisfy two of the boundary conditions, two additional sets $Y^{(4)}$, $Y^{(5)}$, $J^{(4)}$, $J^{(5)}$ etc. would have to be included to satisfy the two boundary conditions at $\rho = \beta$. To obtain a and b, equation (D10) is substituted into the last two of equations (C8), or at $\rho = 1$.

$$\left.\begin{aligned} \left(aL_n^{(1)} + bL_n^{(2)} + L_n^{(3)}\right) + \left(aK_n^{(1)} + bK_n^{(2)} + K_n^{(3)}\right) - (3 - \nu)\left[\left(aJ_n^{(1)} + bJ_n^{(2)} + J_n^{(3)}\right) - \left(aY_n^{(1)} + bY_n^{(2)} + Y_n^{(3)}\right)\right] &= 0 \\ \left(aK_n^{(1)} + bK_n^{(2)} + K_n^{(3)}\right) + \nu\left[\left(aJ_n^{(1)} + bJ_n^{(2)} + J_n^{(3)}\right) - \left(aY_n^{(1)} + bY_n^{(2)} + Y_n^{(3)}\right)\right] &= 0 \end{aligned}\right\} \tag{D11}$$

The starting values for the three solutions that were assumed and that satisfy the boundary conditions at the first station $\rho = \beta$ or $i = 1$ are

$$\left.\begin{array}{lll} Y^{(1)} = 0 & Y^{(2)} = 0 & Y^{(3)} = 0 \\ J^{(1)} = 0 & J^{(2)} = 0 & J^{(3)} = 0 \\ K^{(1)} = 0 & K^{(2)} = 1 & K^{(3)} = 0 \\ L^{(1)} = 1 & L^{(2)} = 0 & L^{(3)} = 0 \end{array}\right\} \quad \text{(D12)}$$

When these starting values are used in the recurrance relations (D8) and (D9), values for Y, J, K, and L can be computed successively for all other stations. Once the values are computed for the last, or n station, the constants a and b are obtained from equations (D11) and the complete solution is then given by equations (D10).

REFERENCES

1. Timoshenko, S.: Theory of Plates and Shells. McGraw-Hill Book Co., Inc., 1940.

2. Manson, S. S.: Determination of Elastic Stresses in Gas-Turbine Disks. NACA Rep. 871, 1947.

3. Hildebrand, F. B.: Introduction to Numerical Analysis. McGraw-Hill Book Co., Inc., 1956.

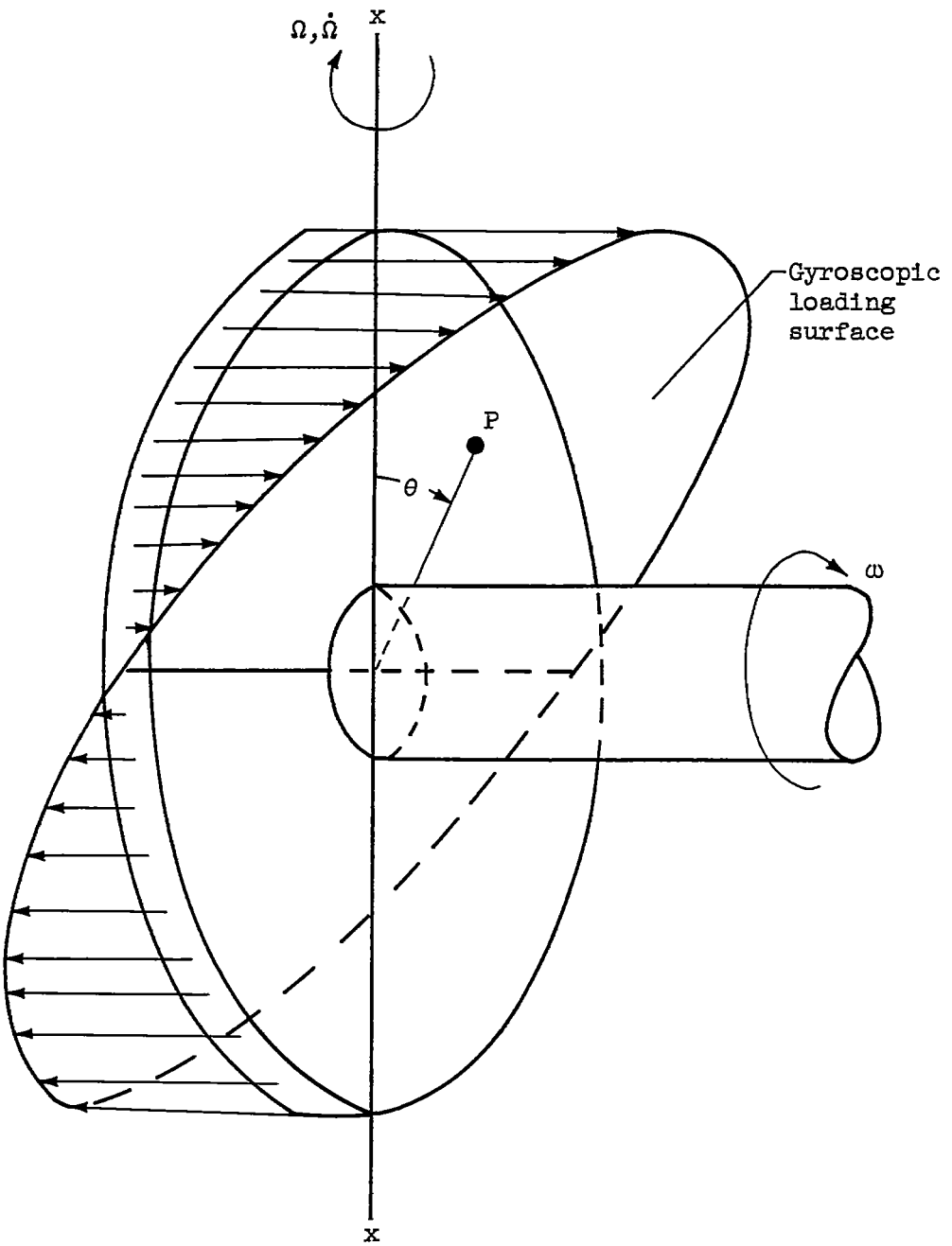

Figure 1. - Loading on disk due to rotation about two axes. Arrow length is proportional to gyroscopic force.

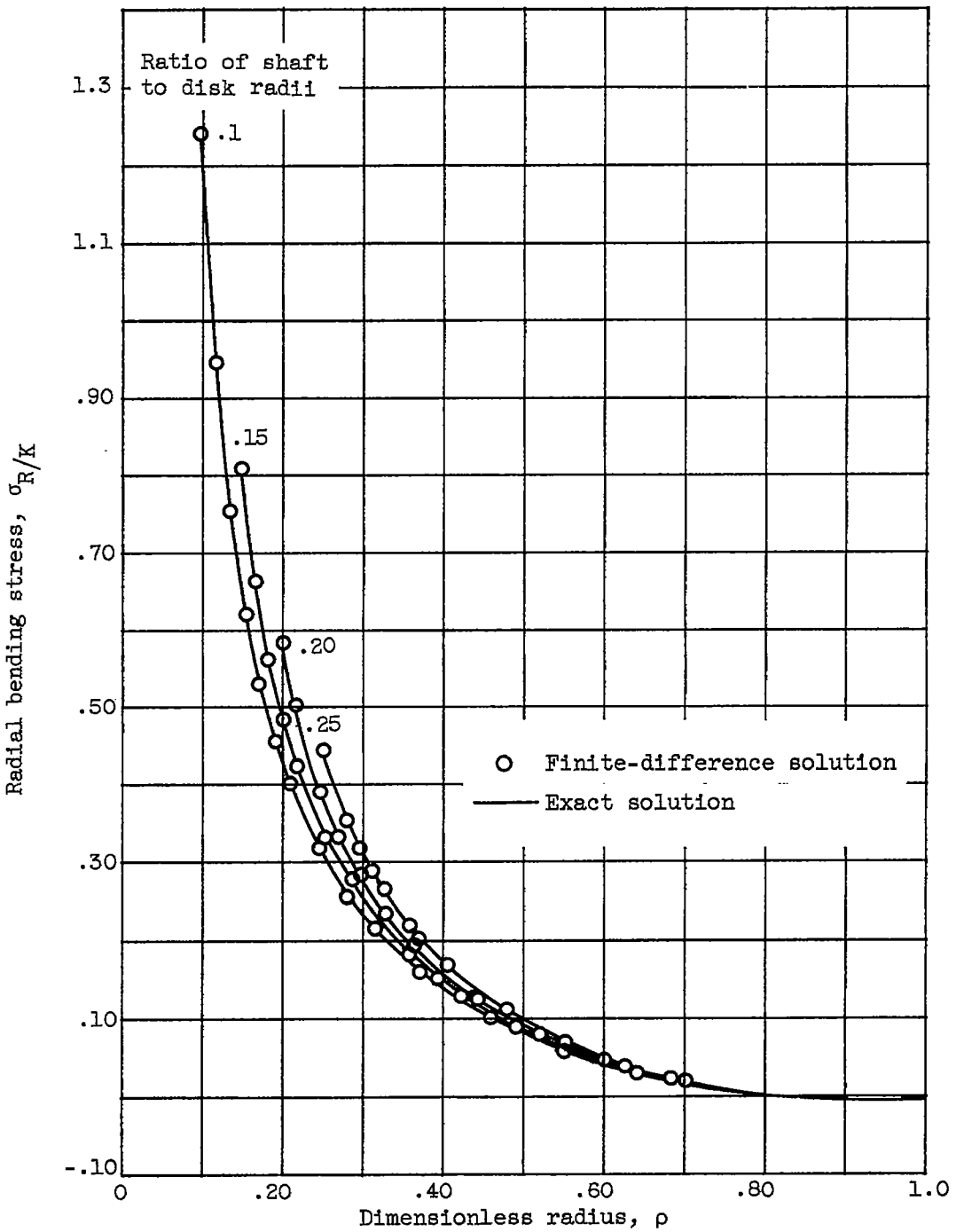

(a) Radial stress.

Figure 2. - Comparison of exact dimensionless stress with stresses obtained by finite difference solution for various ratios of shaft to disk radii. Centrifugal load parameter, zero.

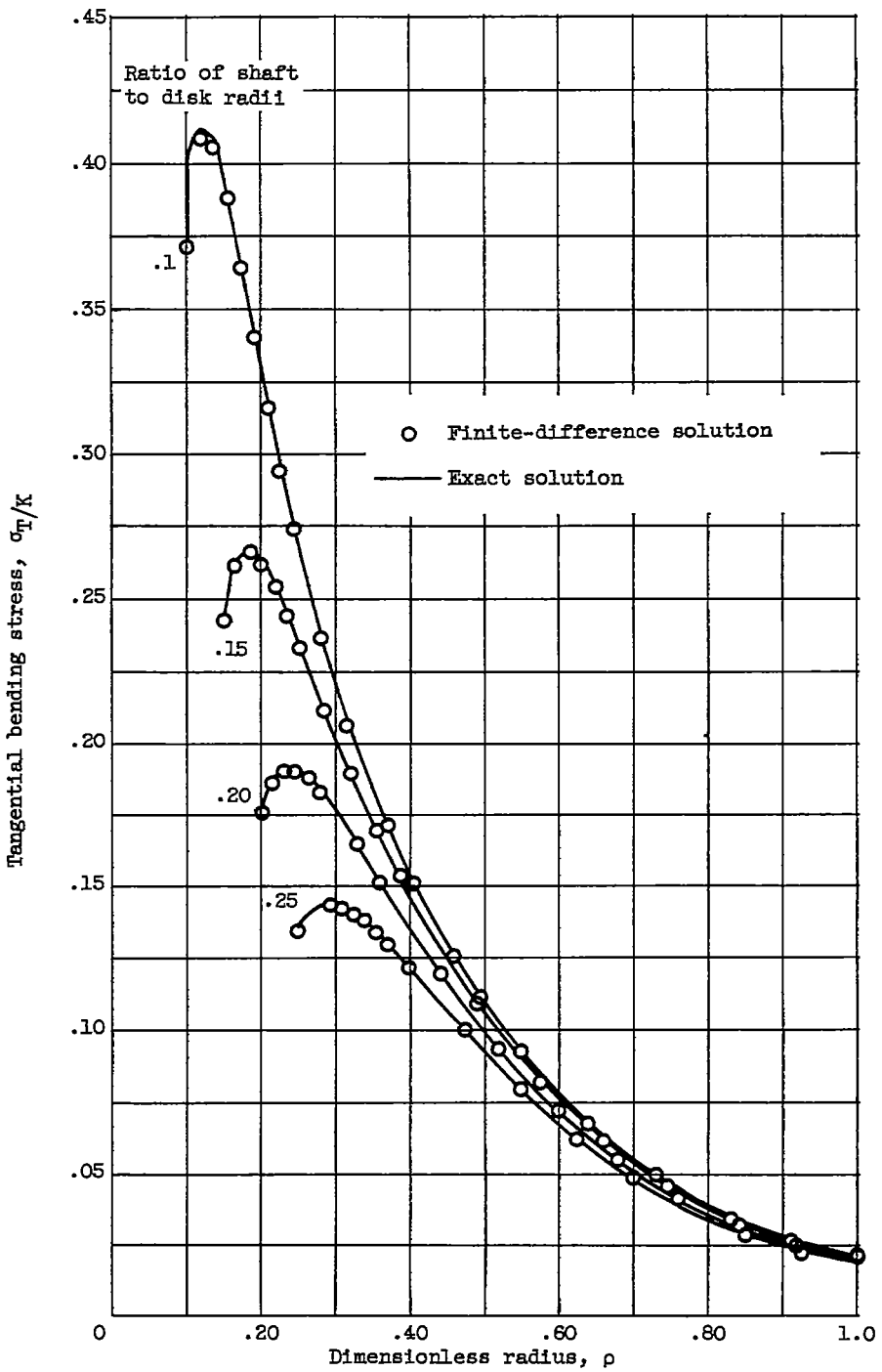

(b) Tangential stress.

Figure 2. - Concluded. Comparison of exact dimensionless stress with stresses obtained by finite difference solution for various ratios of shaft to disk radii. Centrifugal load parameter, zero.

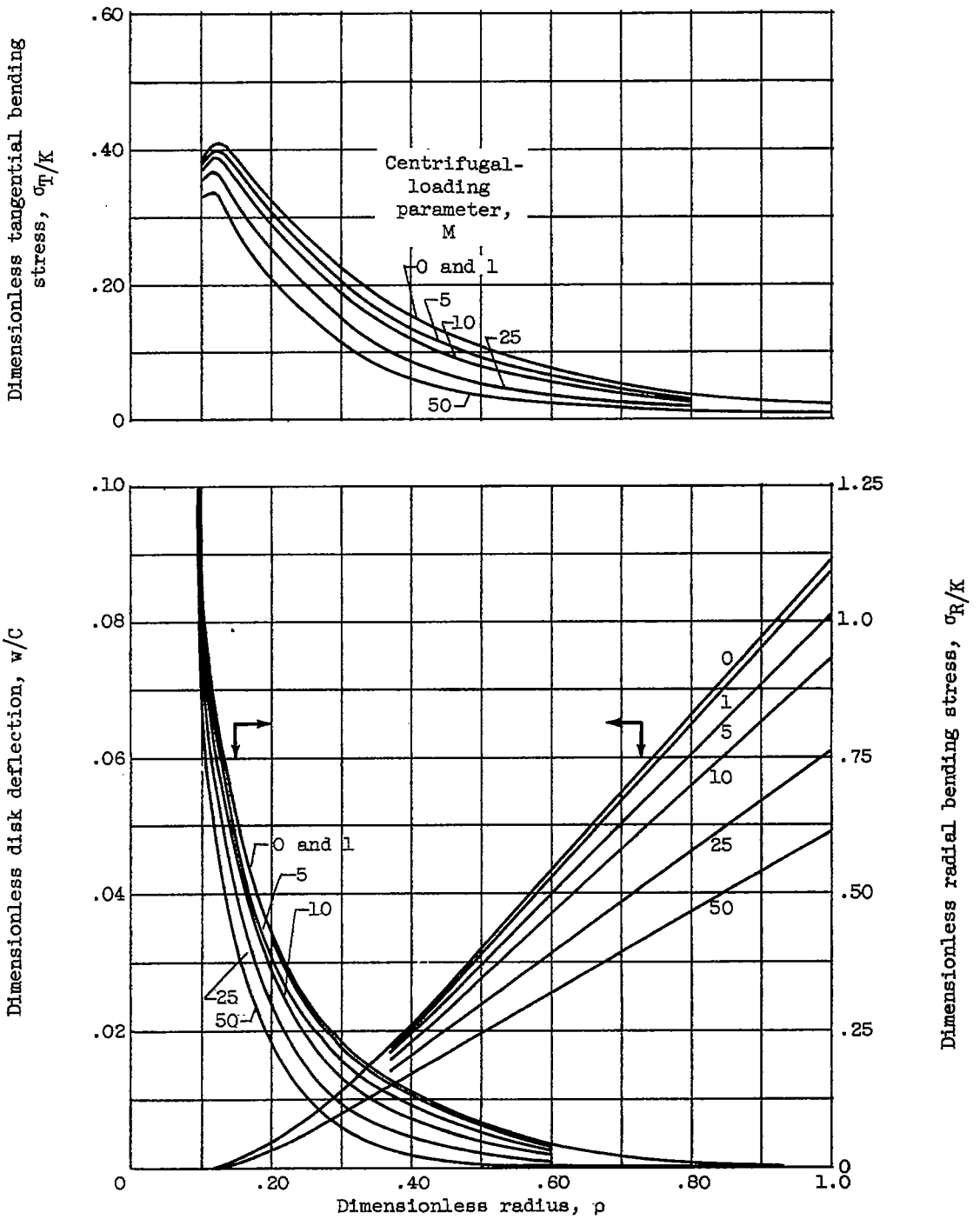

(a) Ratio of shaft to disk radius, 0.100.

Figure 3. - Variation of dimensionless radial stress, tangential stress, and deflection with dimensionless radius for various values of centrifugal loading parameter.

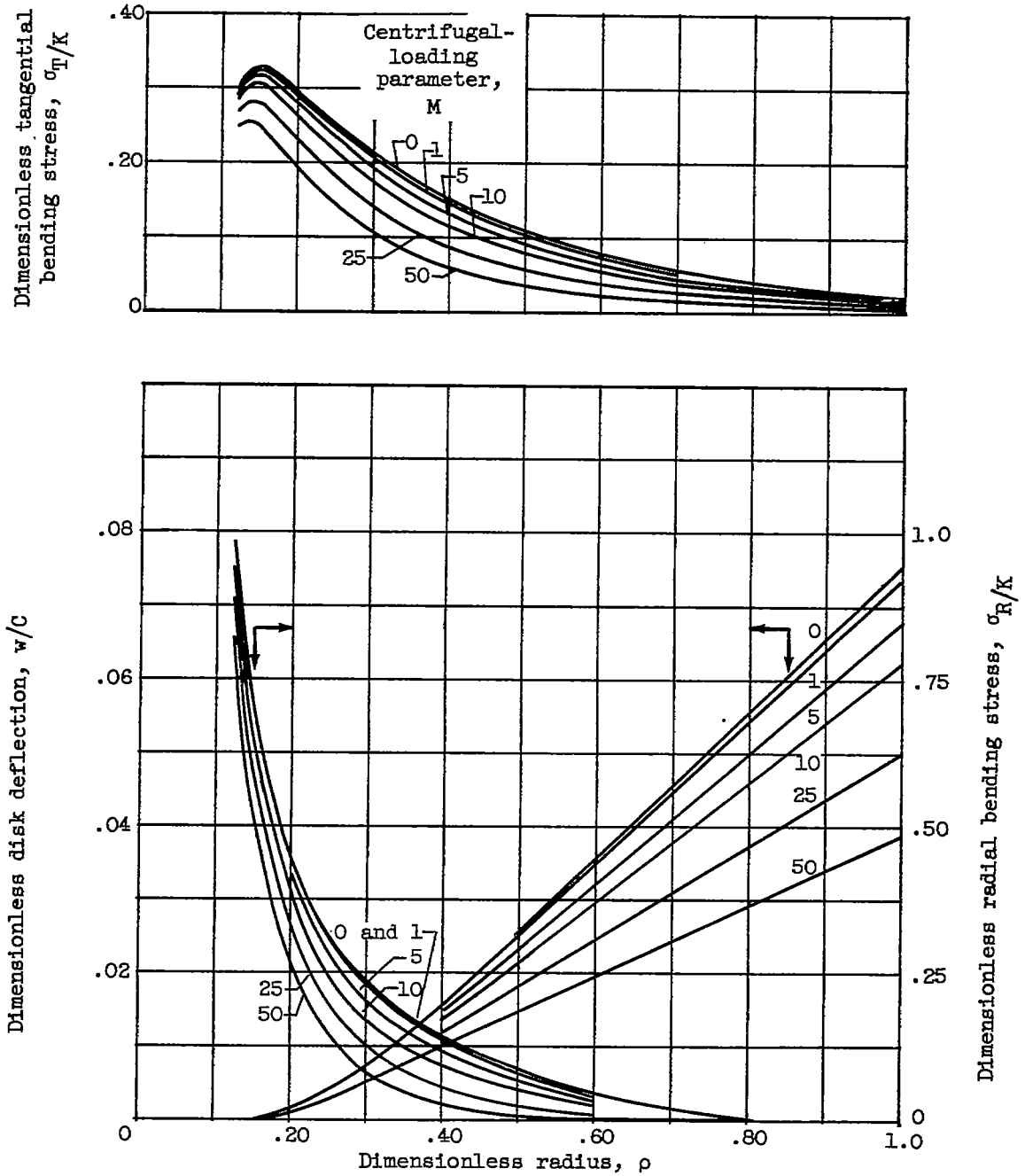

(b) Ratio of shaft to disk radius, 0.125.

Figure 3. - Continued. Variation of dimensionless radial stress, tangential stress, and deflection with dimensionless radius for various values of centrifugal loading parameter.

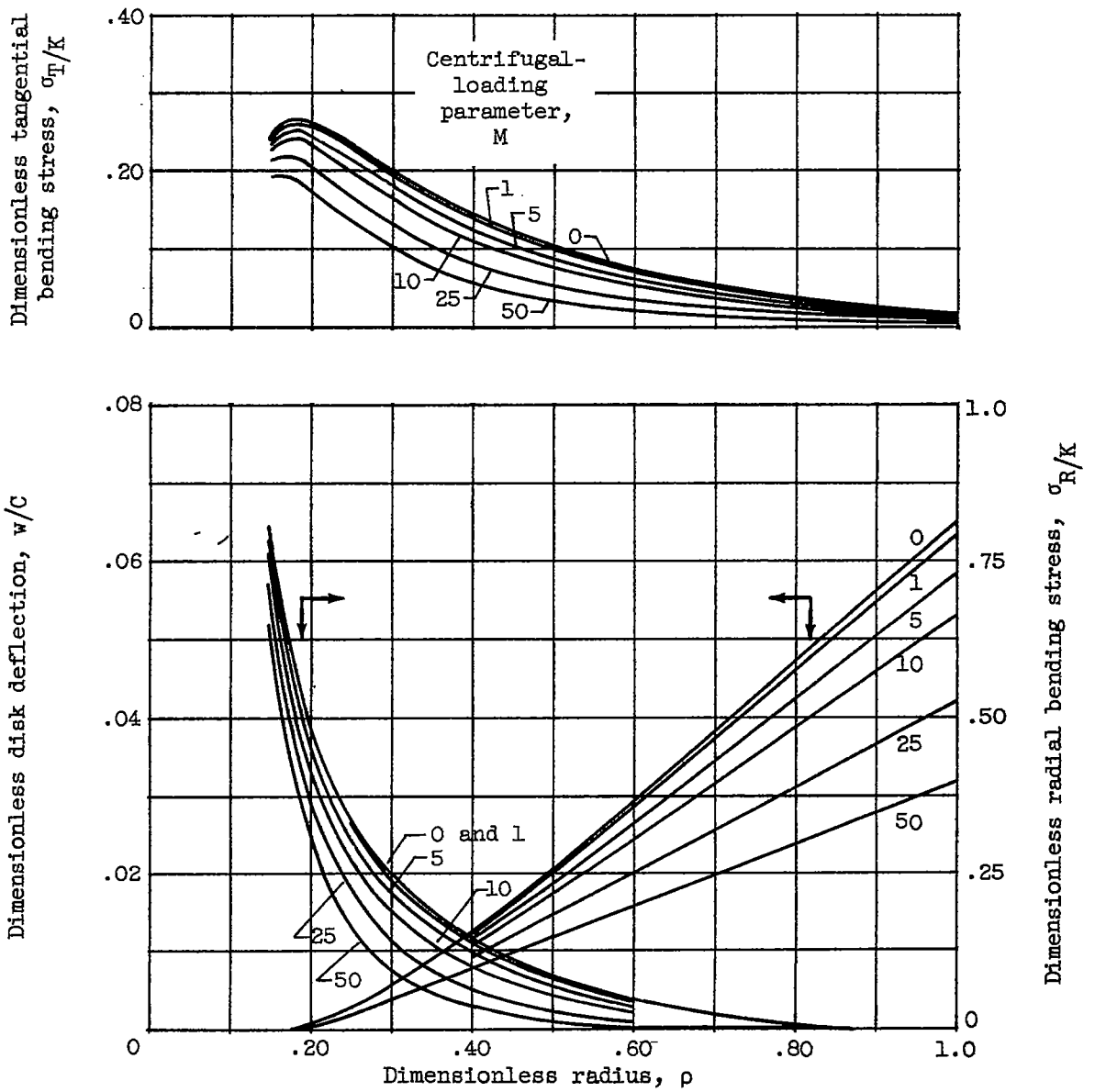

(c) Ratio of shaft to disk radius, 0.150.

Figure 3. - Continued. Variation of dimensionless radial stress, tangential stress, and deflection with dimensionless radius for various values of centrifugal loading parameter.

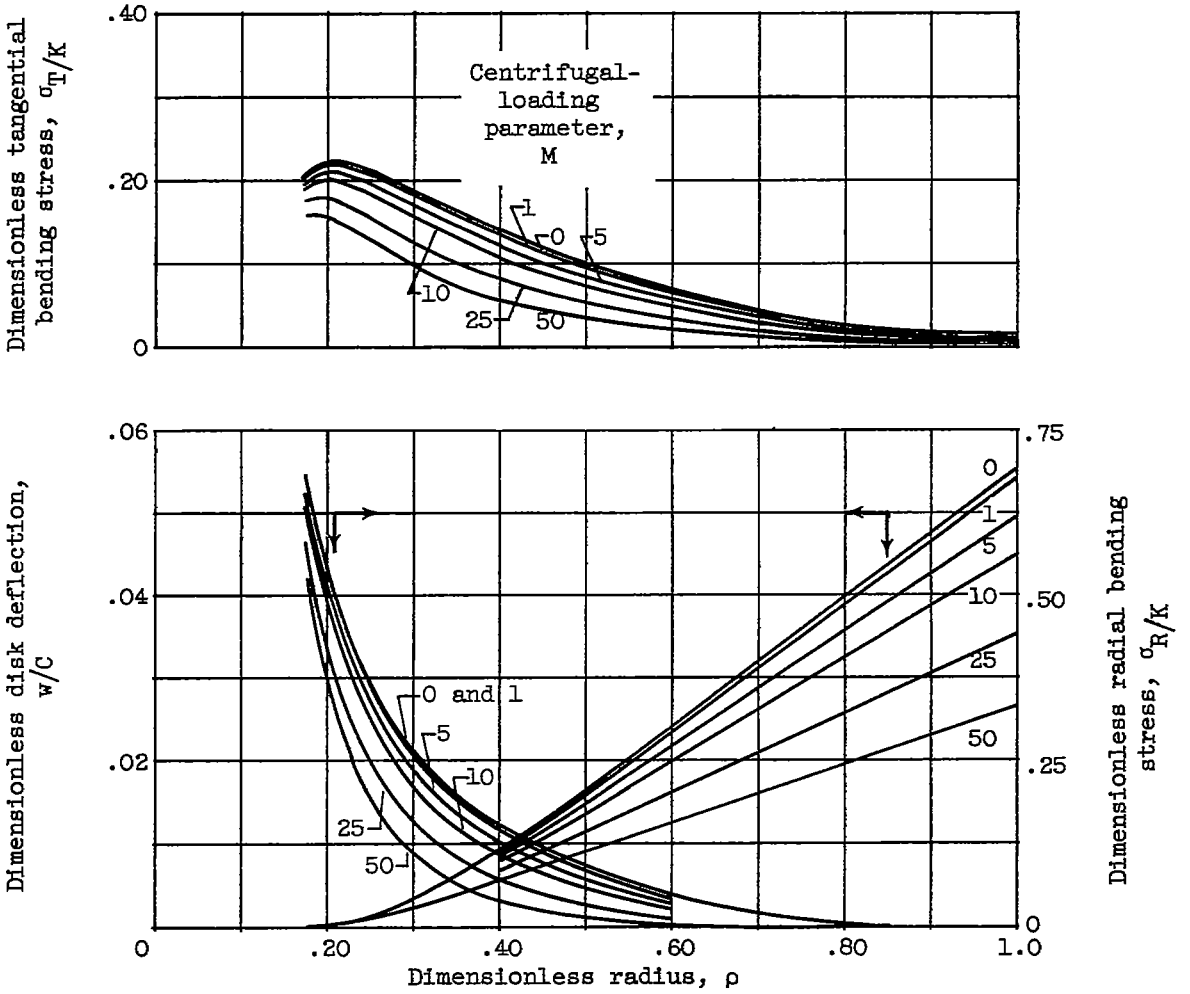

(d) Ratio of shaft to disk radius, 0.175.

Figure 3. - Continued. Variation of dimensionless radial stress, tangential stress, and deflection with dimensionless radius for various values of centrifugal loading parameter.

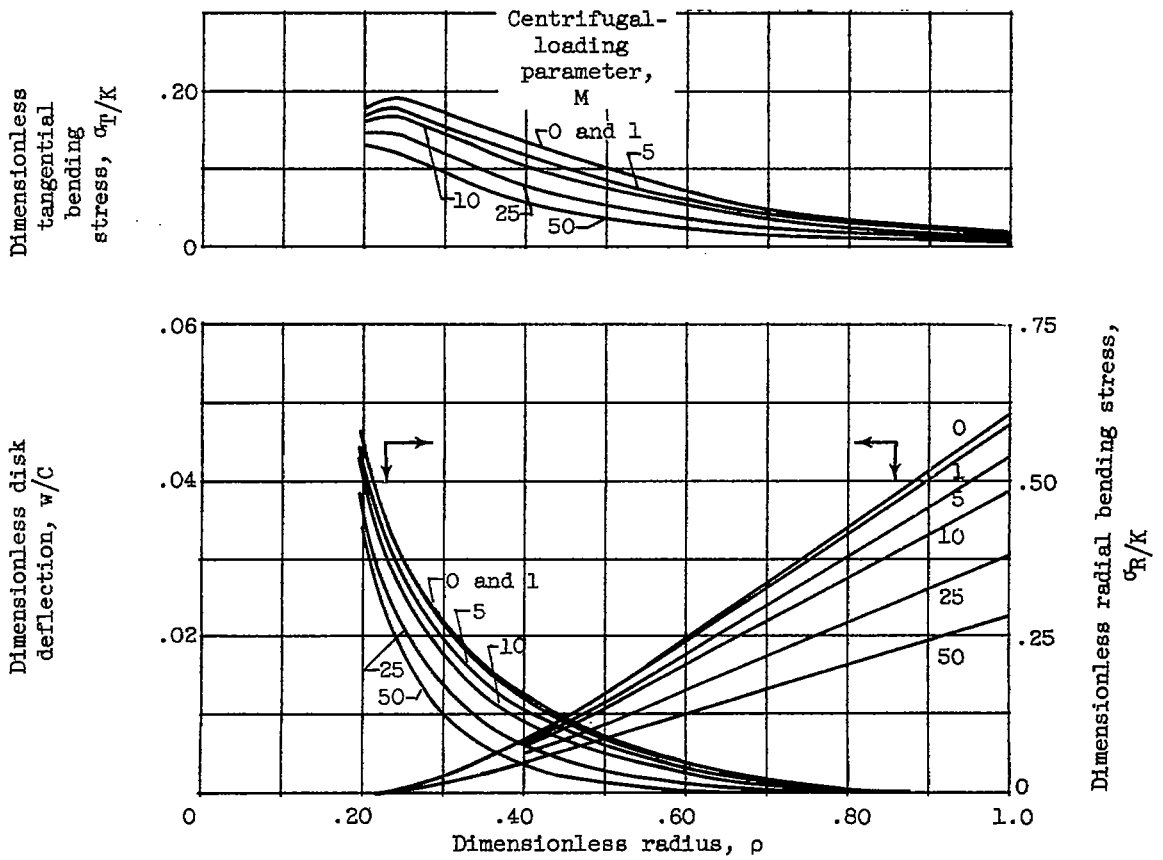

(e) Ratio of shaft to disk radius, 0.200.

Figure 3. - Continued. Variation of dimensionless radial stress, tangential stress, and deflection with dimensionless radius for various values of centrifugal loading parameter.

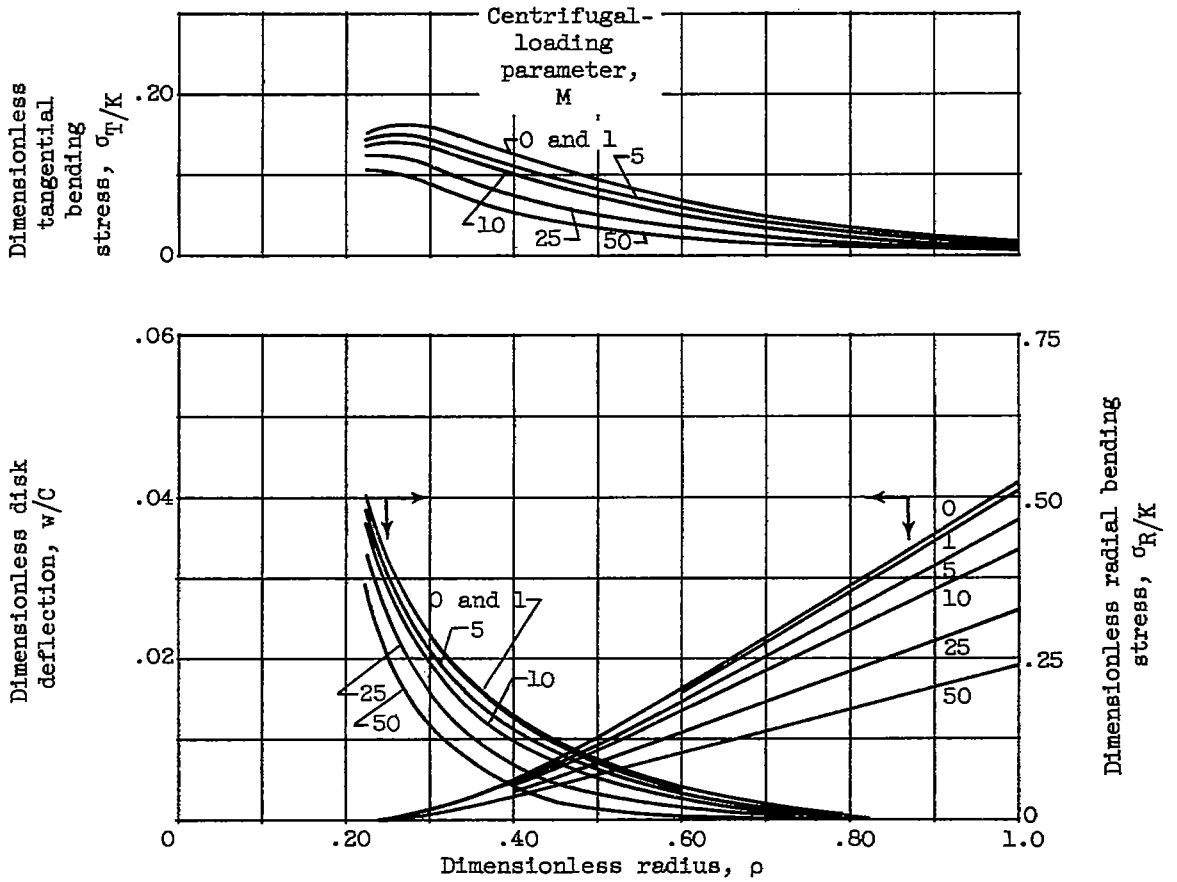

(f) Ratio of shaft to disk radius, 0.225.

Figure 3. - Continued. Variation of dimensionless radial stress, tangential stress, and deflection with dimensionless radius for various values of centrifugal loading parameter.

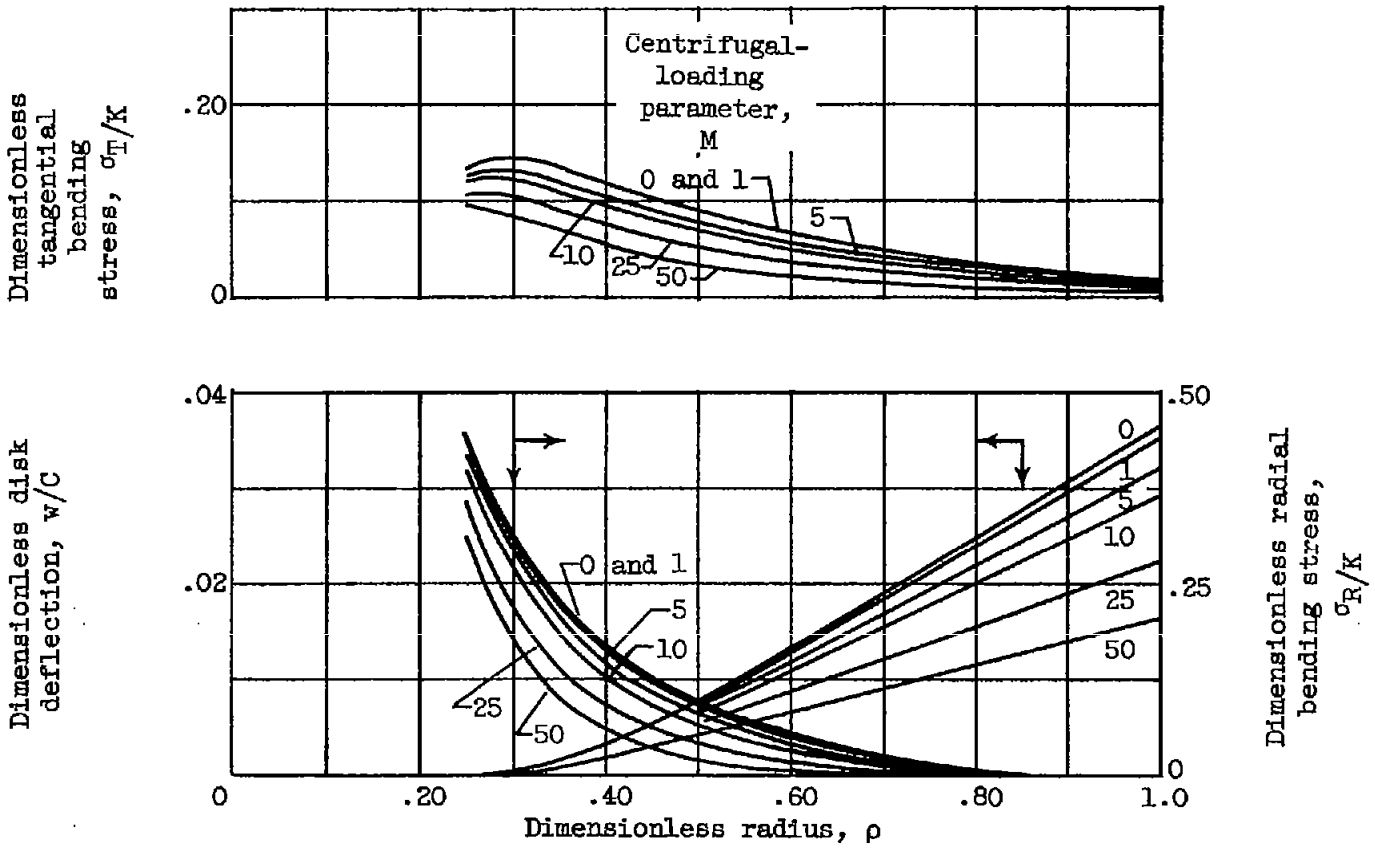

(g) Ratio of shaft to disk radius, 0.250.

Figure 3. - Continued. Variation of dimensionless radial stress, tangential stress, and deflection with dimensionless radius for various values of centrifugal loading parameter.

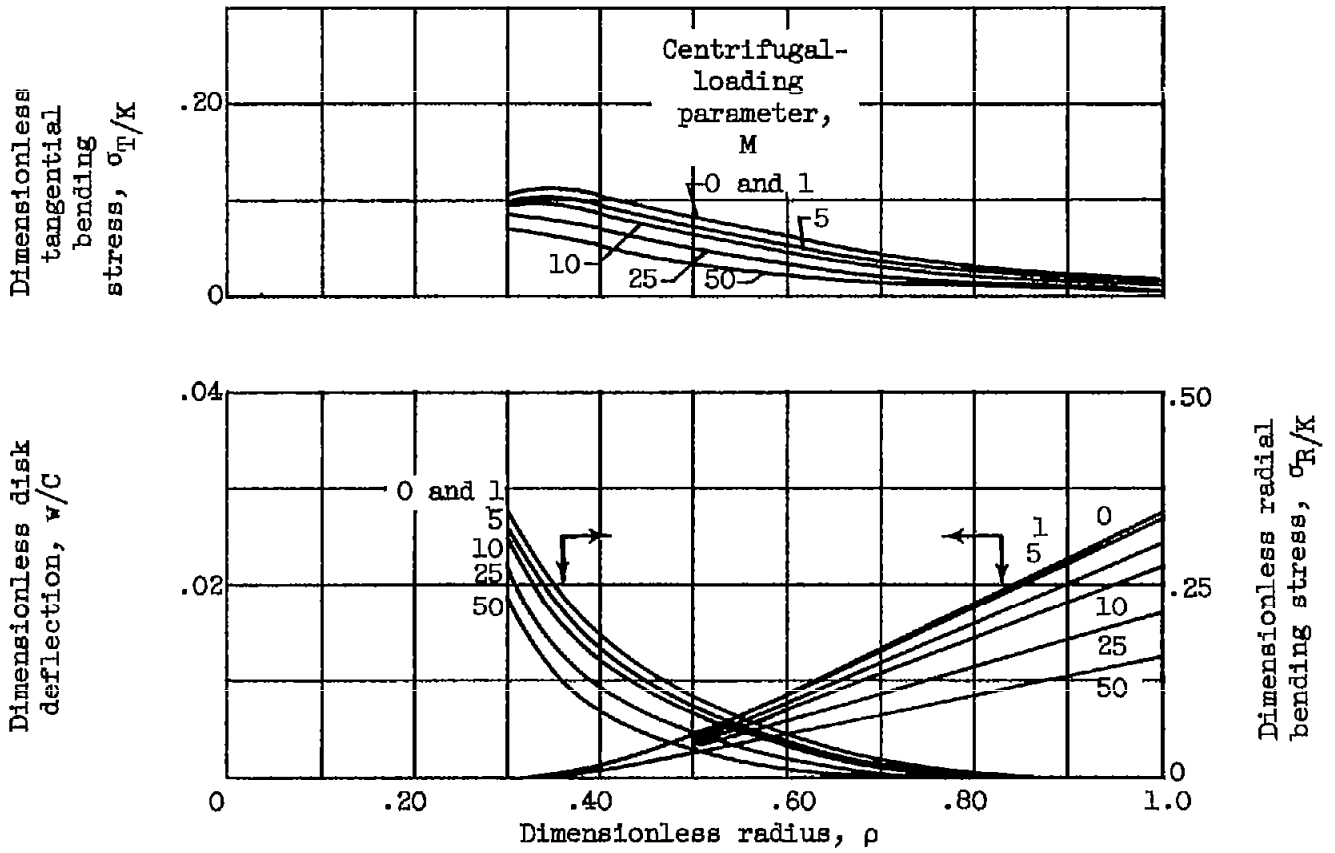

(h) Ratio of shaft to disk radius, 0.300.

Figure 3. - Concluded. Variation of dimensionless radial stress, tangential stress, and deflection with dimensionless radius for various values of centrifugal loading parameter.

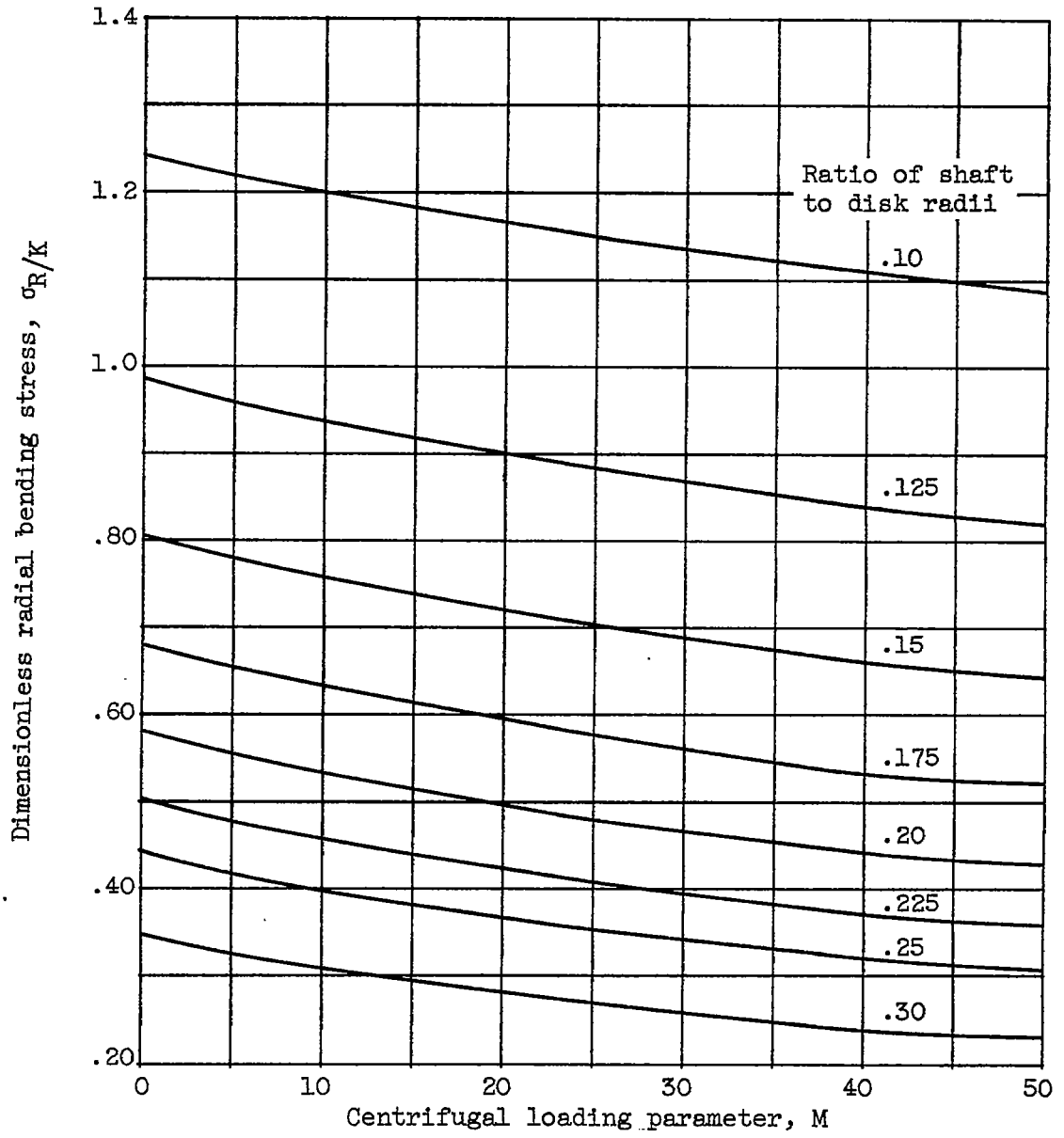

(a) Radial stress.

Figure 4. - Variation of dimensionless stress at shaft with centrifugal loading parameter for various values of ratios of shaft to disk radii.

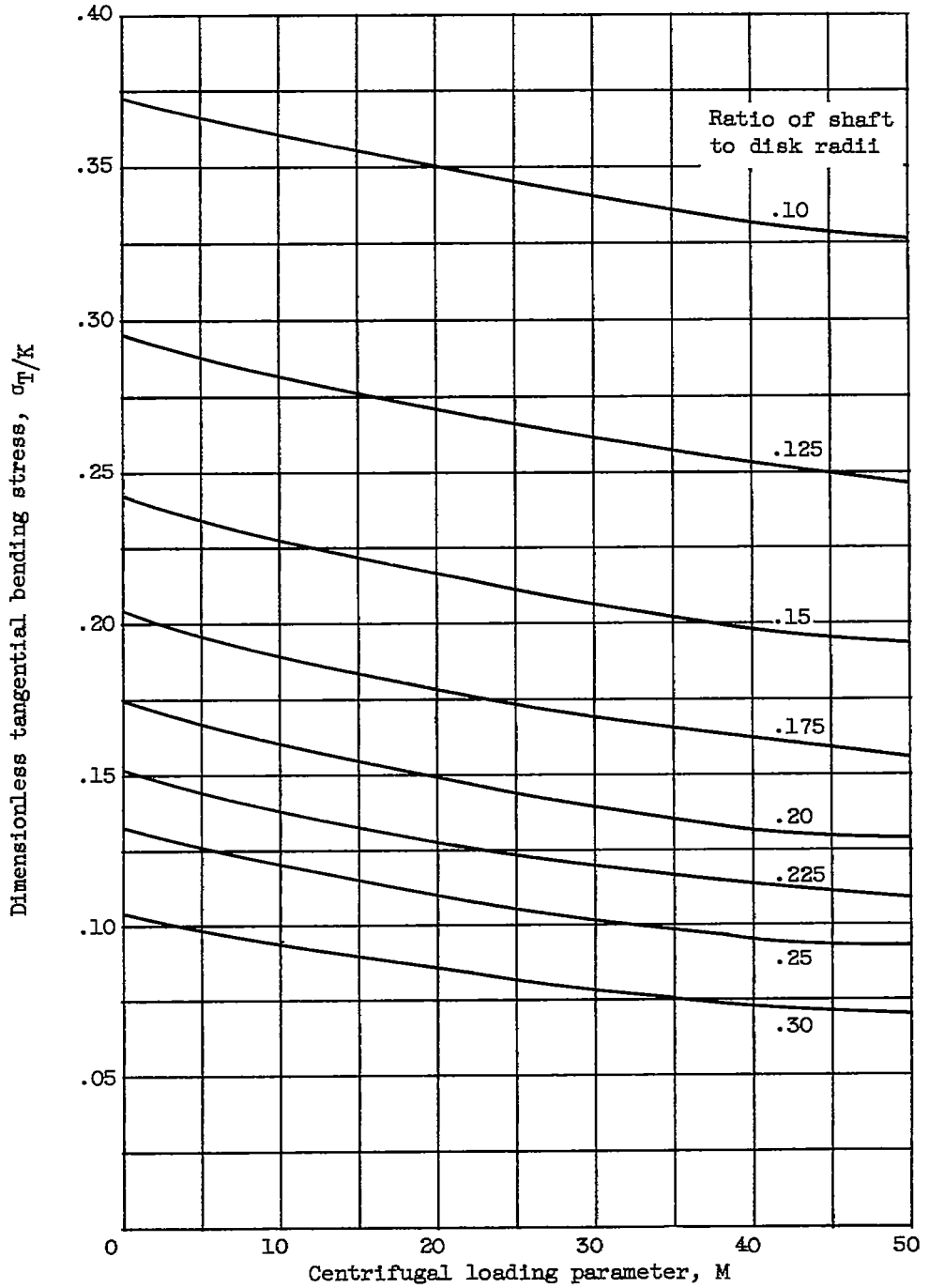

(b) Tangential stress.

Figure 4. - Continued. Variation of dimensionless tangential stress at shaft with centrifugal loading parameter for various values of ratios of shaft to disk radii.

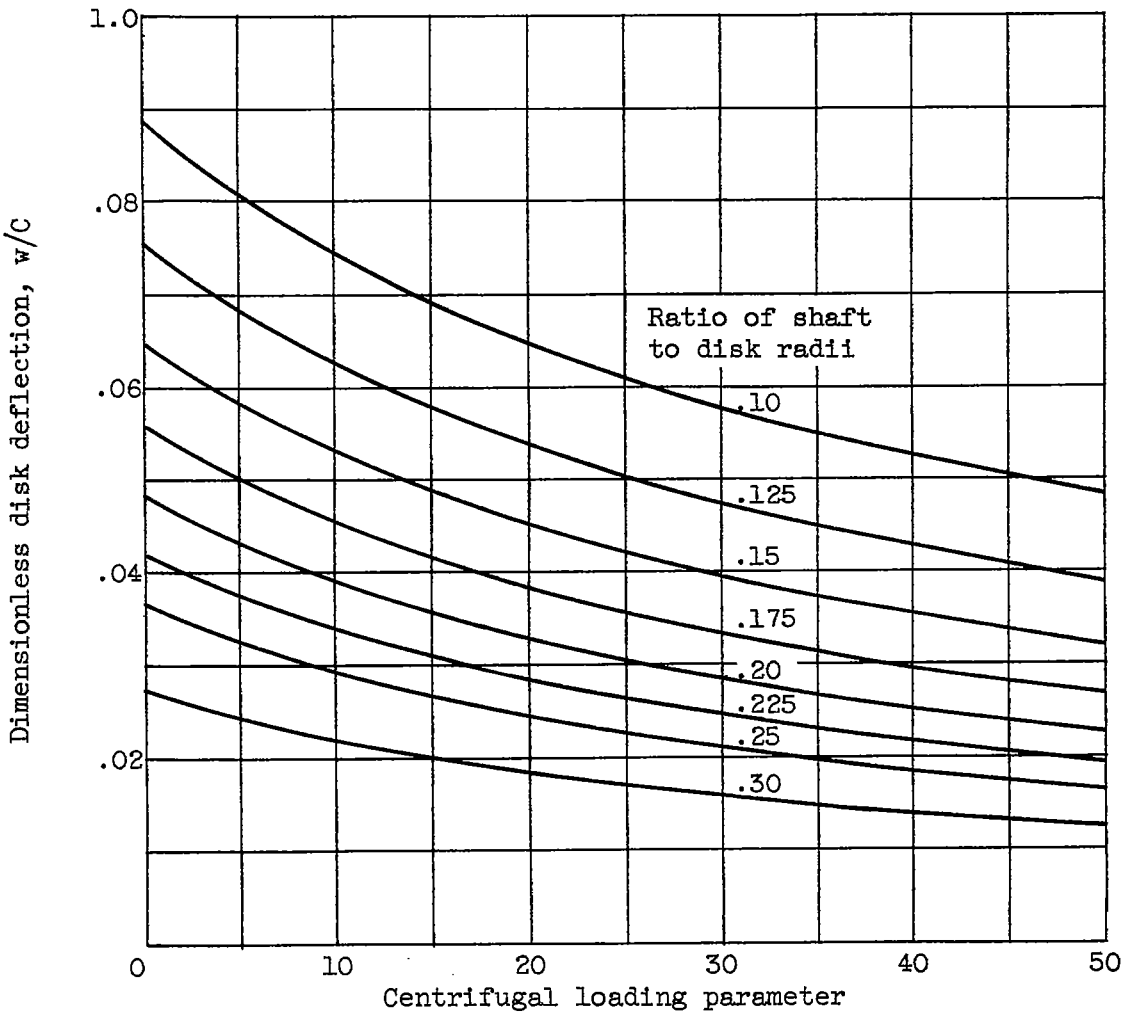

(c) Tip deflection.

Figure 4. - Concluded. Variation of dimensionless stress with centrifugal loading parameter for various values of ratios of shaft to disk radii.

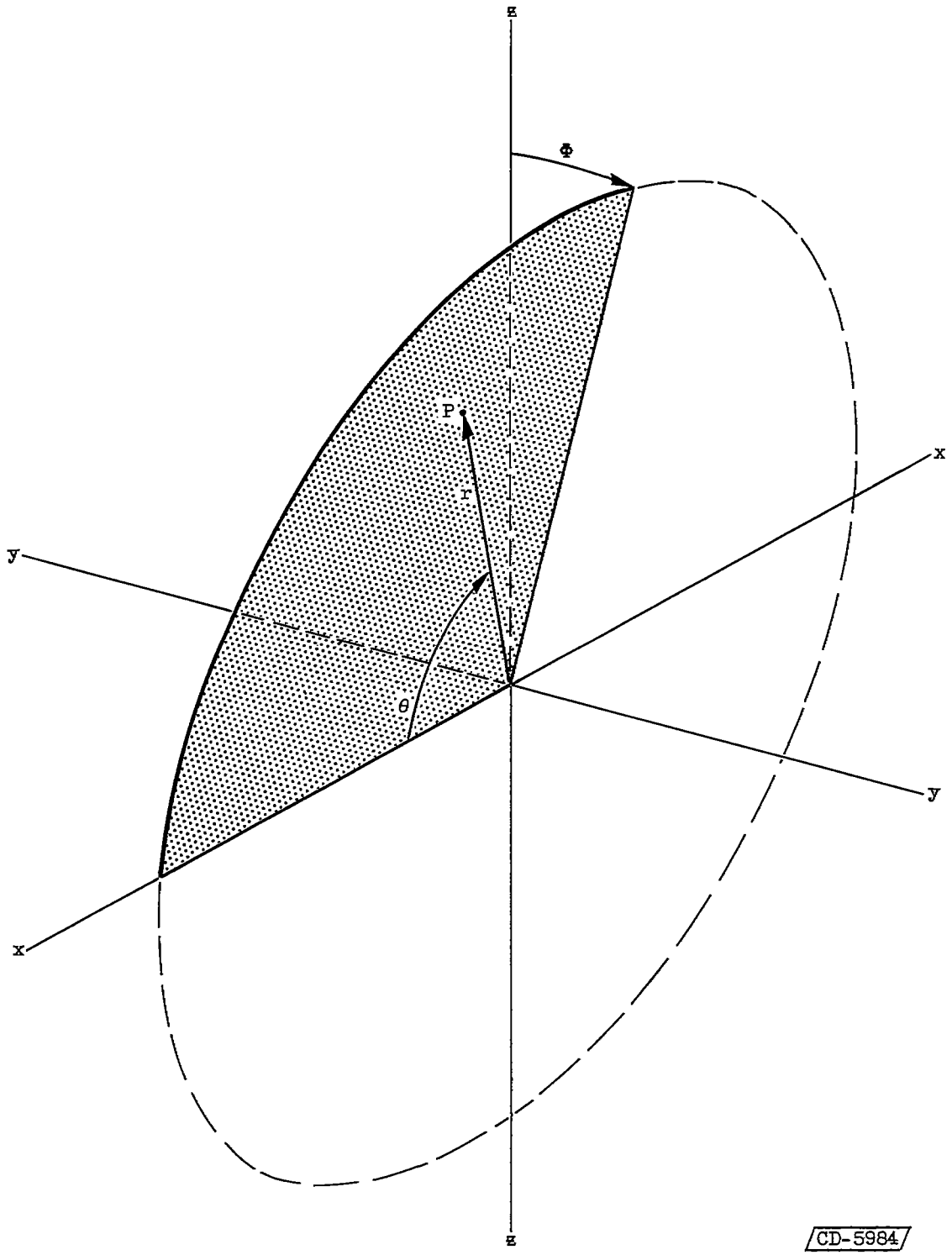

Figure 5. - Coordinate system for calculating acceleration of point P in disk.

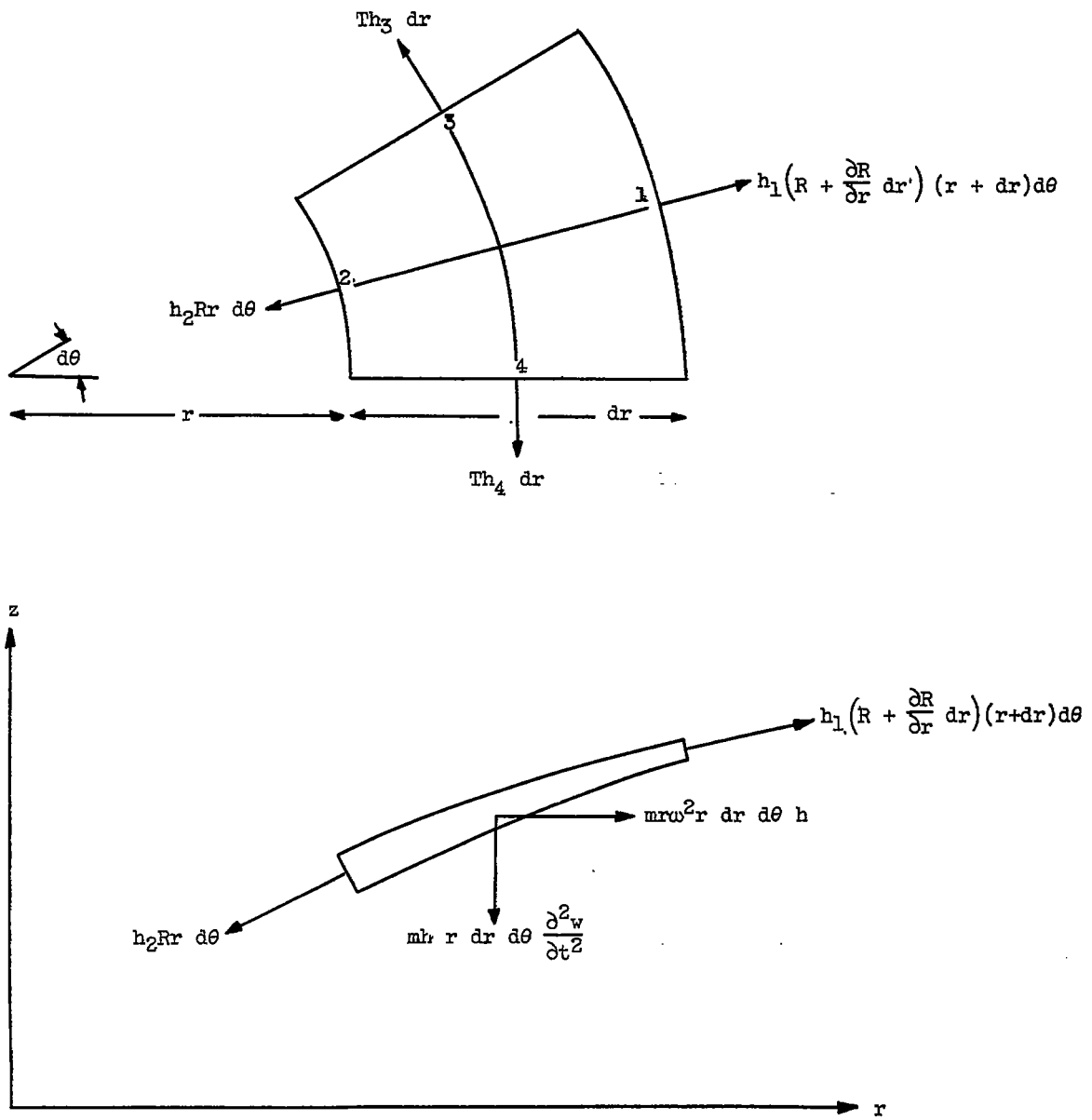

Figure 6. - Equilibrium diagram of disk element.

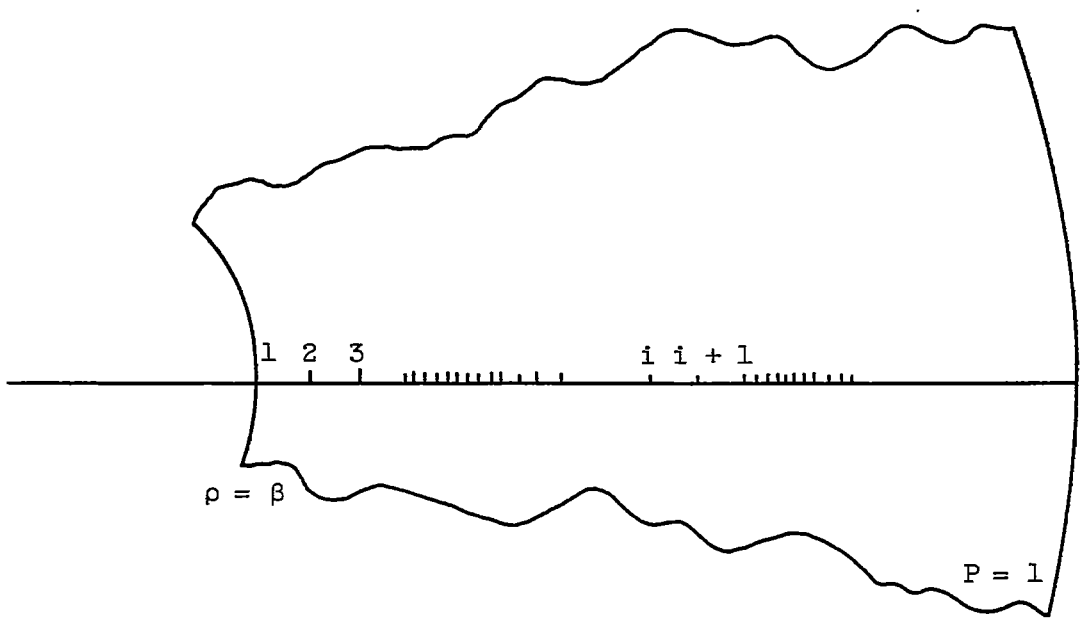

Figure 7. - Section of disk with stations for finite difference equations.